APEM journal
Advances in Production Engineering & Management
Volume 8 | Number 1 | March 2013 | pp 52–60
http://dx.doi.org/10.14743/apem2013.1.153
ISSN 1854-6250
Journal home: apem-journal.org

Influence of laser welding process parameters on weld pool geometry and duty cycle

Tadamalle, A.P.[a,*], **Reddy, Y.P.**[a], **Ramjee, E.**[b]

[a]Department of Mechanical Engineering, Sinhgad College of Engineering, Vadgaon(Bk) Pune, India-411041
[b]Department of Mechanical Engineering, Jawaharlal Nehru Technological University, Kukkatpally, Hyderabad-85

ABSTRACT

In pulsed Nd:YAG laser welding process, the material melts and solidifies consecutively by a peak high power laser beam. The solidification time in this process is very less as compared to that of conventional welding process. The mode of welding process is governed by the process parameters like laser energy, pulse duration, pulse frequency, power and welding speed. This paper aimed at to examine the influence of welding speed and power on weld bead geometry and performance parameters such as duty cycle, pulse overlap, energy density and bead diameter. In this contest, first experiment is conducted on austenitic 304L stainless steel sheet by varying the welding speed from 2 mm/s to10 mm/s and second experiment is conducted varying laser power from 300 W to 3500 W. It was found from the experimental and analytical approach welding speed and laser power significantly affects on weld bead geometry, variation in bead diameter from pulse to pulse, duty cycle and effective pulse energy.

ARTICLE INFO

Keywords:
Duty cycle
Pulse overlap
Effective pulse energy

**Corresponding author:*
Ashok_p_t@yahoo.com
(Tadamalle, A. P.)

1. Introduction

The success of laser welding depends on the careful consideration of process parameters and its requirements. The effective laser material processing is often useful to get a theoretical estimation of expected process results. The heating of sheet metal with a laser beam require knowledge about the expected rise in temperature of the work piece. The rise in temperature has effect on weld bead geometry, weld velocity, gas flow rate, work piece hardness and microstructure. Many researchers have carried out investigation to deal with the estimation of weld bead geometry, heat affected zone, hardness and microstructure. Balasubramaniam et al. [1] investigated that beam power and welding speed are the major process parameters influencing on depth of penetration and bead width. The most significantly affecting process parameter leads to an acceptable weld quality and efficiency. The resultant tensile and impact properties of the weld joint were correlated with the weld metal microstructure. Codigo Do Trabalho [2] has carried out investigation to examine the influence of weld joint gap on 304L stainless steel using Nd:YAG laser welded joints to characterize weld bead geometry. It was found that butt joint welds are sensitive to gap and the gap tolerances which in turn is dependent on material thickness, beam diameter, welding speed and beam quality. Balasubramaniam et al. [3] conducted experiments using three level Box Behnken's method to analyze transient temperature profiles, weld pool geometry, bead width using SYSWELD software in 304 stainless steel sheets and optimized weld parameters such as power, welding speed and beam angle for deep penetration.

Ramesh Singh et al. [4], characterized and estimated effect of temperature distribution on heat affected zone in laser assisted micro grooving process. The HAZ generated by laser heating of steel at different laser scanning speeds is analyzed for change in microstructure and micro hardness. The results are correlated with heat affected zone and critical temperature.

Hector L. G. et al. [5], have done investigation on characterization of the microstructure texture in the weld zone during Nd:YAG laser welding process has been carried out at selected depths along the weld line. Lee et al. [6] have characterized with higher fusion zone depth to width ratio, cooling rate and porosity amount during laser beam welding process by varying power, welding speed and focal position. The effect of different inert gases on weld line appearances, fusion zone dimensions, solute evaporation, micro hardness, post weld tensile properties and porosity distribution has been studied. It was found that the increases heat input, the fusion zone area and depth/width ratio shows increasing trend. Masoumi M. et al. [7] investigated the effect of pulse frequency, laser energy and weld speed on mechanical and metallurgical characterization of low carbon steels and found that effective pulse energy is the controlling factor for determination of weld joint strength. Nath, A. K. et al. [8] investigated the amount of heat required to melt the substrate in welding process using experimental results, dimensionless parameter model and energy balance model. Paleocrassas A. G. et al. [9] have investigated and found the optimum welding speed was between 2 and 3 mm/s for maximum penetration of 1.02 mm by defining effluence and weld energy per weld length by taking power, speed and focal length in consideration. Yi Chun Liao and Ming Huei Yu [10], investigated that effect of incident angle on depth of penetration, bead width and bead length and found that depth of penetration and bead width increases and bead length decreases with increase in incident angle.

Zhang Y. M. et al. [11] discussed about important information which contained weld pool as a welding process consequence. The same author [9] proposed polar coordinate model to characterize and measure weld pool geometry online with the help of neural network. Khan M. M. A. et al. [12], investigated that depth of penetration is directly proportional to the welding speed. The welding speed increases bead width decreases and depth/ width ratio increase. Yoshiyaki Arata et al. [13], developed new mathematical model to bead depth in high density laser beam and found that as the bead diameter increases progressively, initially bead width remains constant and then increases gradually. Chang W. S. [14] has calculated depth of penetration using various heat source equations that have been proposed in various studies were compared the predictions with the proposed model. The many researchers have conducted experiments to characterize the heat affected zone, weld bead geometry and other process related parameters, but the effect of process parameters on pulse overlap, duty cycle, Pulse off time, pulse energy have not tried. This paper aimed at to carry out experimental and analytical investigation to predict the effect of welding speed and laser power on weld pool geometry and performance parameters such as duty cycle, energy density, pulse off time and pulse overlap.

2. Estimation of performance parameters

In this section the different performance parameters related to Nd:YAG laser welding process is described.

2.1 Estimation of overlapping factor and duty cycle

The pulse overlap is measured by using image analyzer. The sample results of bead on plates created at welding speeds of 2 mm/s and 10 mm/s are as shown in Fig. 2(a) and Fig. 2(c), respectively. The overlapping factor is computed by equation 1 suggested by Masoumi et al. [7].

$$\text{Overlapping factor} = \left[1 - \frac{\left(\frac{v}{f}\right)}{(D + v \cdot t)}\right] \cdot 100 \tag{1}$$

$$OT = (1 - Overlap\%) \cdot \left(\frac{b}{v}\right) \tag{2}$$

$$DC = \left[1 - \frac{PD}{(PD + OT)}\right] \tag{3}$$

where *f*, *t*, *v* and *D* corresponds to the frequency, sheet thickness, welding speed and bead diameter, respectively. The duty cycle is a rating factor that indicates how long a machine can be used at its maximum output without affecting the performance of the machine. The laser welding machine may overheat if the duty cycle is exceeded. Paleocras and Grant [9] suggested equation 2 to compute pulse off time *OT* and equation 3 to compute duty cycle *DC*.

The duty cycle can be increased and the power source can be used for a longer period of time at lower input parameters like welding speed and power.

2.2 Estimation of effective pulse energy

The effective pulse energy *EPE* is a factor which shows the actual energy input to the material per unit area. A fraction of the total energy supplied from laser source is retained in the specimen, as a result of which a small area of the underlying material melts. The laser power and welding speed determine the energy input rate to the work piece. The energy density *E* is estimated by equation 4.

The effect of energy density on number of pulse overlap *n*, overlapping factor *F* and the effective pulse energy is estimated by equations 5a to 5c proposed by Masoumi et al. [7].

The EPE is a key factor for assessing the mechanical strength of weld joint. An increase in effective pulse energy promotes sputtering on the weld surface as shown in Fig. 4(d).The EPE leads to an undesired failure mode with reduced peak load and energy absorption.

3. Experimental procedure

The 304L austenitic stainless steel has been selected for the investigation, because of its many advantages over other materials such as low thermal conductivity, high resistance to corrosion, high stability at elevated temperatures and superior absorber of laser energy. The chemical composition and mechanical properties of 304L stainless steel is presented in Table 1. The experiments have been carried out on 0.5 mm and 1.2 mm thick sheets. The sheets are cleaned and cut into rectangular specimens of 30 mm × 50 mm with the help of wire cut electric discharge machine to avoid the distortion.

The schematic diagram of Nd:YAG Laser welding setup shown in Fig. 1. The Nd:YAG laser source is used to deliver laser beam with a maximum capacity of 4 kW in multimode condition. The plane polarized laser beam comes out of the laser source. The beam delivery system consists of phase retarder which converts laser beam from plane polarized to circularly polarized form. The mirror acts as a beam bender and focusing lens are used to focus laser beam on the work piece. A separate nozzle is used for deliver the argon gas to prevent work piece from oxidation and heat dissipation. The CNC part program co-ordinates both table movements and laser power delivery control.

$$E = \frac{p}{(v \cdot D)} \tag{4}$$

$$n = D \cdot \frac{f}{v} \tag{5a}$$

$$F = 1 + 2n\left[1 - \left(\frac{(n+1)v}{2fD}\right)\right] \tag{5b}$$

$$EPE = E \cdot F \tag{5c}$$

Table 1 Chemical composition

C	Mn	Ni	Cr	Si	V	N
0.3 %	2.0 %	8–12 %	18–20 %	0.75 %	0.07 %	0.1 %
	Proof stress		Yield strength		Elongation	
	170 MPa		485 MPa		40 %	

The laser welding is carried out by placing the specimen on machine bed and held firmly by means of permanent magnets on either side of the plates. The specimen mounting arrangement used for creating bead on plate during the welding process is shown in Fig. 2. The first set of experiment is conducted on 0.5 mm thick stainless steel sheet by varying the welding speed from 2 mm/s to 10 mm/s and the second set of experiment is conducted on 1.2 mm thick sheet by varying laser power from 300 W to 3500 W. The process parameters and thermo-mechanical properties used during the welding and computation are given in Table 2 and Table 3, respectively.

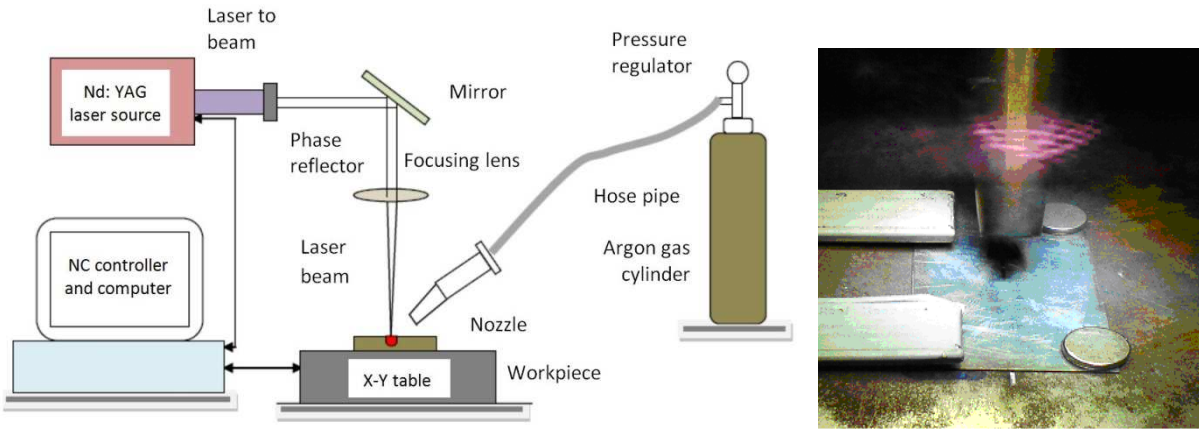

Fig. 1 Specimen mounting arrangement

3.1 Effect of process parameters on weld bead geometry

The welding experiments were conducted to study the effect of welding speed, energy density, power density, pulse off-time and duty cycle on weld bead geometry and pulse overlap by varying the welding speed from 2 mm/s to 10 mm/s. The weld samples were cut into transverse directions and the cross sectional surfaces are prepared for metallographic inspection according to ASTM-G48 standards. The welded joints ware polished by using different grade polishing papers and then specimens are etched by using electrolytic etching process to observe the weld bead geometry and microstructure. The samples prepared for metallographic inspection are as shown in Fig. 2(a) to Fig. 2(d). The measurement of weld bead geometry parameters are carried out by using an optical microscope and image analyzer. The weld samples are examined for heat affected zone and found that the heat affected zone is not a straight line along the weld direction as shown in Fig. 2(a) and Fig. 2(c). This is due to inhomogeneity of base material, fluctuation in power and machine process capabilities.

Table 2 Process parameters

Parameters	Values	Parameters	Values
Gas flow rate	7 l/min	Pulse energy	2.76 J
Pulse duration	4 ms	Spot diameter	0.4 mm
Frequency	25 Hz	Focal distance	150 mm
Beam angle	90 ± 0.5 °		

Table 3 Thermo mechanical properties of the 304L stainless steel

Parameters	Values	Parameters	Values
Density	8030 kg/m^3	Poisons Ratio	0.29
Elastic modulus	193 GPa	Melting point	1723 K
Mean coefficient of expansion	18.4 µm/(m·°C)	Refractive index	3.81 Fe
Thermal conductivity	20 W/(m·K)	Enthalpy	8.7 J/mm^3
Specific heat	500 J/(kg·K)	Diffusivity	5.7 mm^2/s

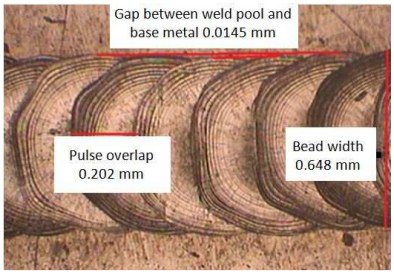

(a) Top view (2 mm/s)

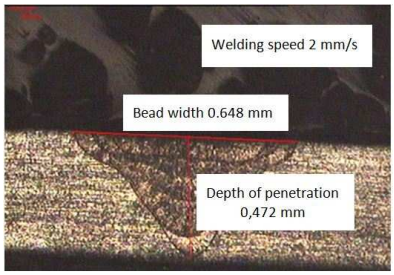

(b) Traverse cross section (2 mm/s)

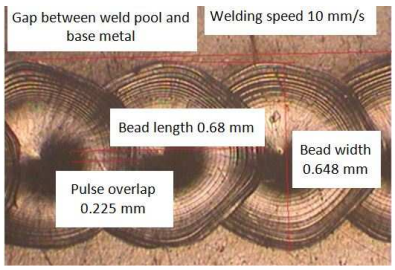

(c) Top view (10 mm/s)

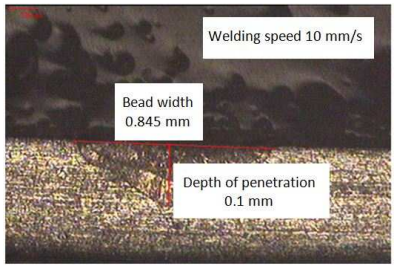

(d) Transverse cross section (10 mm/s)

Fig. 2 Transverse cross section and top views of welded joints

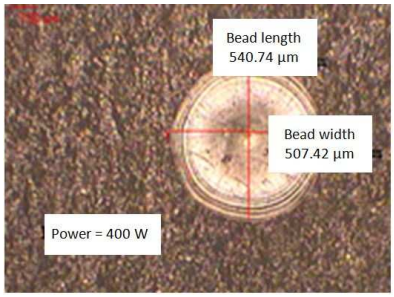

(a) At 400 W

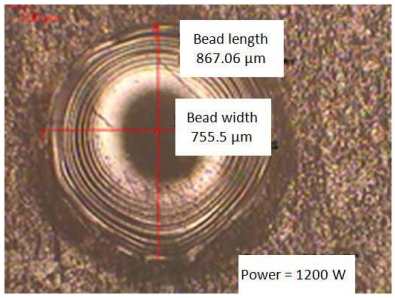

(b) At 1200 W

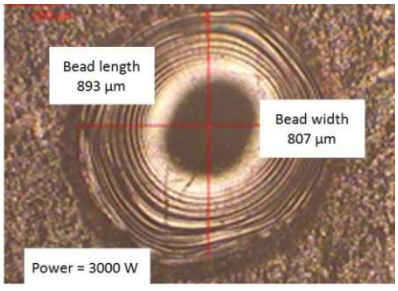

(c) At 1800 W

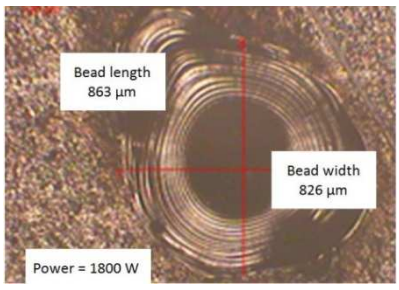

(d) At 3000 W

Fig. 3 Bead width and bead length created at different laser powers

The weld beads are created on 1.2 mm austenitic stainless steel sheet with single laser pulse by varying the pulse power from 300 W to 3500 W in steps of 100 W. The weld pool dimensions have been measured with the help of image analyzer. Fig. 3 shows the weld pool geometry pho-

tographs created by supplying pulse laser power input of 400 W, 1200 W, 1800 W and 3000 W, respectively.

The photographic inspection shows that power input increases which results in increase in the weld bead dimensions and promotes spattering. Spattering in welds ultimately results into reduction in the strength of the weld joint.

4. Results and discussions

Fig. 4 shows that bead width and depth of penetration are the function of speed. The bead width and depth of penetration decreases as welding speed increases. The result predicts that the depth of penetration is more sensitive to the welding speed than bead width. This is due to decrease in the amount of heat input and less interaction time period between laser beam source and the weld material.

Fig. 5 shows that bead width and bead length are directly proportional to the power up to 1700 W. The size of the bead width and bead length increases over the range of 300–1700 W of power and beyond 1700 W power it is observed that the fluctuation in the dimensions weld bead geometry lies within a range of 30 μm. It is observed in all consecutive spots the bead length is greater than bead width. This is due to variation in the angle of incidence of laser beam and high heat input.

The effect of depth of penetration on duty cycle is shown in Fig. 6. The depth of penetration and pulse off time has linear relationship up to 98.38 % of its duty cycle, beyond this value depth of penetration decreases drastically from 0.375 mm to 0.1 mm over the range of 0.62 % of duty cycle. Duty cycle has significant effect on weld bead geometry and whereas duty cycle is directly proportional to pulse off time.

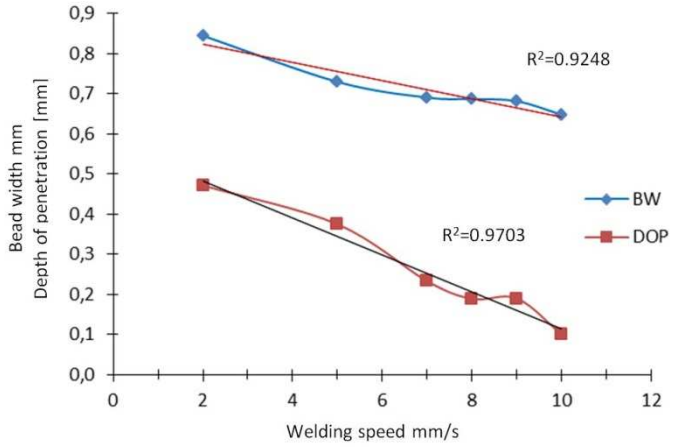

Fig. 4 Effect of welding speed on bead width and depth of penetration

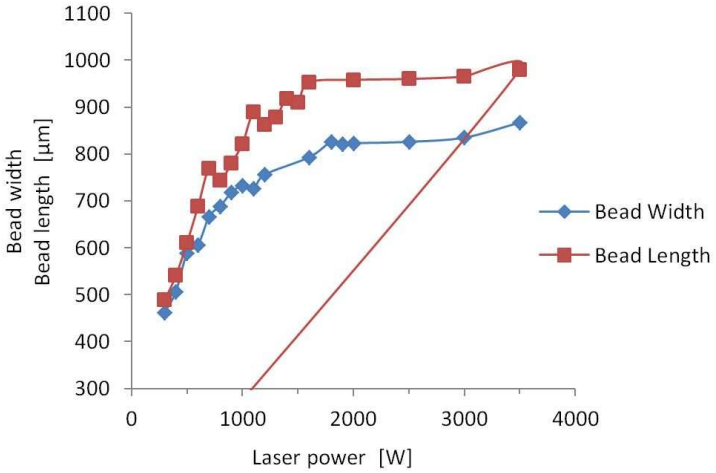

Fig. 5 Effect of average laser beam power on bead width and bead length

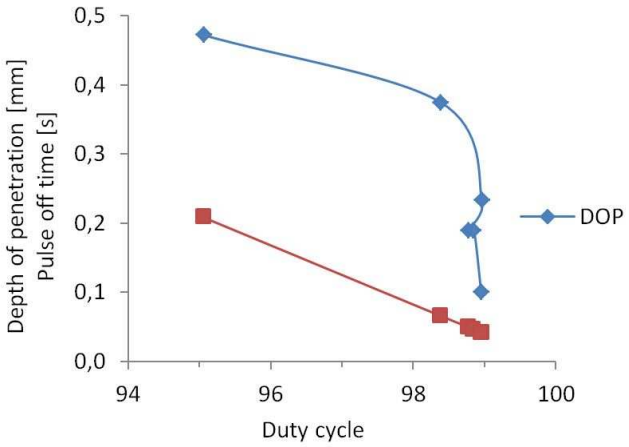

Fig. 6 Relation between duty cycle, depth of penetration and pulse off time

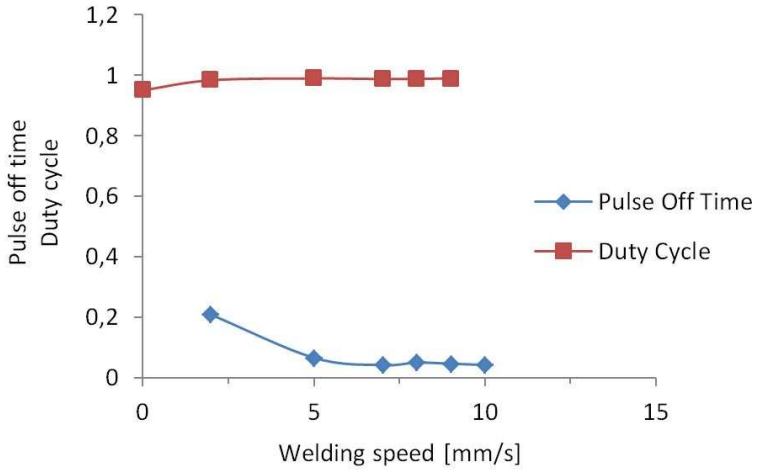

Fig. 7 Effect of welding speed on duty cycle and pulse off time

Welding speed has less significant effect on duty cycle as compared to the bead width and depth of penetration. Fig. 7 reveals that the maximum variation of 3.9 % and 0.013 % in duty cycle and pulse off time, respectively, over a selected range of 2–10 mm/s of welding speed.

Fig. 8 shows the percentage of pulse overlap increases and overlapping factor decreases up to the welding speed of 7 mm/s. The variation in pulse overlap beyond 7 mm/s is less significant and this range provides low strength and quality of weld.

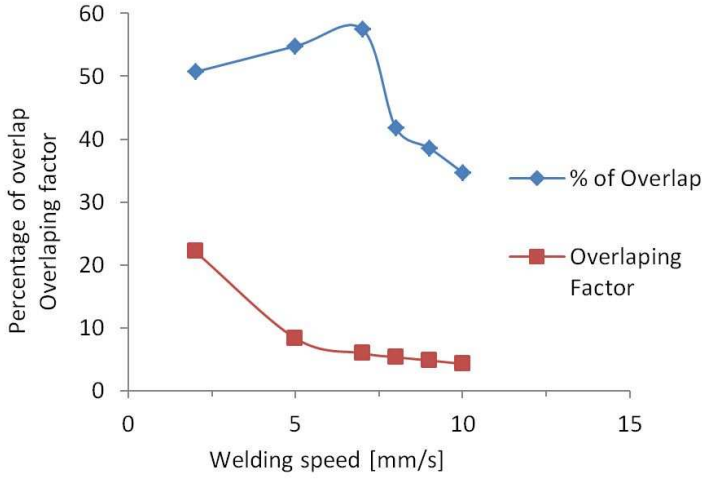

Fig. 8 Effect of welding speed on percentage of overlap and overlapping factor

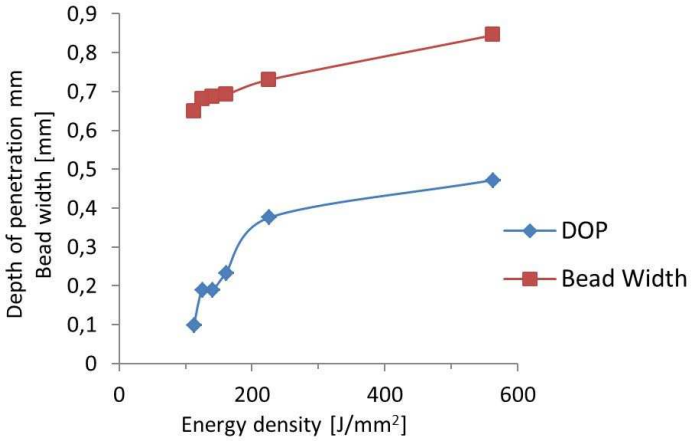

Fig. 9 Effect of energy density on weld bead geometry

Fig. 9 depicts that up to 225 J/mm^2 of energy density, it is directly proportional to bead width and depth of penetration and beyond this value it has been found that 0.0002 mm variation in the bead width and depth of penetration. The full depth of penetration will occur beyond 600 J/mm^2 of energy density. Initially up to 225 J/mm^2 of energy density the depth of penetration increases drastically from 0.1 mm to 0.375 mm and thereafter the value of depth of penetration increases from 0.375 mm to 0.472 mm for the additional energy input of 337 J/mm^2. The laser energy input to the specimen become quite larger over a small area which results in increase in the depth of penetration and bead width. This can be reduced to a certain extent by fixing the job tightly.

The effective pulse energy input to the specimen decreases with the increases in the value of welding speed as shown in Fig. 10. The Effective pulse energy input is directly proportional to the welding speed up to 5 mm/s and beyond this the effective pulse energy decreases gradually from 13.8 J to 6.9 J over a span of 5 mm/s. This may be due to decrease in heat input, because of reduction in exposure period of laser beam with weld material.

The analytical and experimental investigation shows that welding speed increases as the effective pulse energy input to the work piece decreases within the investigation range, which in turn, decreases the melting ratio.

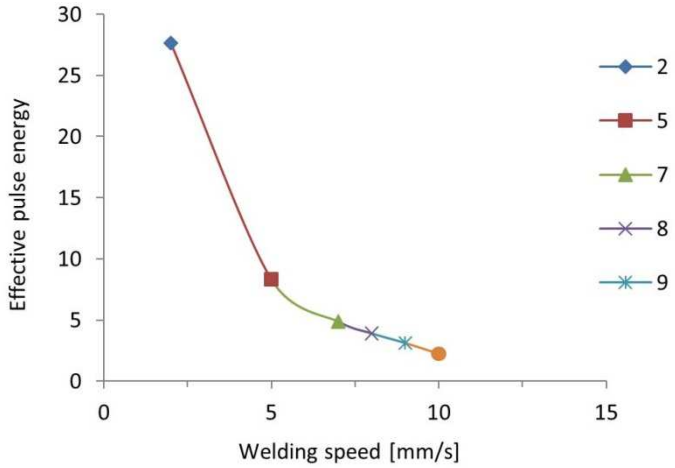

Fig. 10 Effect of welding speed on effective pulse energy

5. Conclusion

Weld bead geometry, effective pulse energy, energy density, duty cycle, percentage of overlap and pulse off time have been analyzed. The bead width, depth of penetration decreases as the welding speed increases, depth of penetration is more sensitive to the welding speed than bead width over range of speed selected for the study. The weld bead dimensions are more sensitive to the peak power input up to 1700 W and less sensitive beyond 1700 W. Laser welding machine can't be loaded beyond 98.38 % of duty cycle. Further this work can be extended to study the effect of shielding gas, pulse duration and focal position on duty cycle, weld bead geometry and process efficiencies.

Acknowledgement

We acknowledge the BCUD, University of Pune for providing the financial support to carry out this research work wide sanction letter no. BCUD/OSD/184/2009-10/03. We also thanks to the M/S Trumpf, Hinjewadi, pune for providing facility to conduct experiments.

References

[1] Balasubramanian, K. R., Buvanashekaran, G., Sankaranarayanasamy, K. (2010). Modeling of laser beam welding of stainless steel sheet butt joint using neural networks, *CIRP Journal of Manufacturing Science and Technology*, Vol. 3, No. 1, 80-84.

[2] Codigo Do Trabalho: 021018171. (2009). Characterization of Nd:YAG pulsed laser welded austenitic AISI 304L stainless steel, V congresso brasileiro de engenharia de fabricação 14 a 17 de abril de 2009, Belo Horizonte, Minas Gerais, Brasil. Online http://www.ipen.br/biblioteca/2009/eventos/14600.pdf.

[3] Balasubramanian, K. R., Siva Shanmugam, N., Buvanashekaran, G., Sankaranarayanasamy, K. (2008). Numerical and experimental investigation of laser beam welding of 304 stainless steel, *Advances in Production Engineering and Management*, Vol. 3, No. 2, 93-105.

[4] Singh, R., Alberts, M. J., A., Melkote, S. N. (2008). Characterization and prediction of the heat-affected zone in a laser-assisted mechanical micromachining process, *International Journal of Machine Tools and Manufacturing*, Vol. 48, No. 9, 994-1004.

[5] Hector, L. G., Chen, Y. L., Agarwal, S., Briant, C. L. (2004). Texture characterization of autogenous Nd:YAG laser welds in AA5182-O and AA6111-T4 aluminum alloys, *Metallurgical and Materials Transactions,* Vol. 35, No. 9, 3032-3038.

[6] Lee, M. F., Huang, J. C., Ho, N. J. (1996). Micro structural and mechanical characterization of laser-beam welding of a 8090 AL-Li thin sheet, *Journal of material science*, Vol. 31, 1455-1468.

[7] Masoumi, M., Marashi, S. P. H., Pouranvari, M. (2010). Metallurgical and Mechanical characterization of laser spot welded low carbon steel sheets, *Steel research international*, Vol. 81, No. 12, 1144-1151.

[8] Nath, A. K., Sridhar, R., Ganesh, P., Kaul, R. (2002). Laser power coupling efficiency in conduction and keyhole welding of austenitic stainless steel, *Sadhana*, Vol. 27, Part 3, 383-392.

[9] Paleocrassas, A. G. (2009). Process characterization of low speed, fiber laser welding of AA 7075-T6 – application to fatigue crack repair, A dissertation submitted to the Graduate Faculty of North Carolina State University, in partial fulfilment of the requirements for the Degree of Doctor of Philosophy. Online: http://www.lib.ncsu.edu/resolver/1840.16/4796.

[10] Liao, Y. C., Yu, M. H. (2007). Effect of laser beam energy and incident angle on the pulse laser welding of stainless steel thin sheet, *Journal of materials processing technology*, Vol. 190, No. 1-3, 102-108.

[11] Zhang, Y. M. Kovacevic, R.; Li, L. (1996). Characterization and real time measurement of geometrical weld pool shape, Int. *Journal of mech. Tools manufacturing*, Vol. 36, No. 7, 799-816.

[12] Khan, M. M. A., Romoli, L., Fiaschi, M., Dini, G., Sarri, F. (2011). Experimental design approach to the process parameter optimization for laser welding of martensitic stainless steel in a constrained overlap configuration. *Optics and Laser Technology*, Vol. 43, No. 1, 158-172.

[13] Arata, Y., Miyamoto, I. (1972). Theoretical analysis of weld penetration due to high energy density beam, *Transaction of AWRI*, Vol. 1, 11-16.

[14] Chang, W. S., Na, S. J. (2002). A study on prediction of the laser weld shape with varying heat source equations and the thermal distortion of a small structure in micro-joining, *Journal of materials processing technology*, Vol. 120, No. 1-3, 208-214.